Sequential bifurcations in sheared annular electroconvection

Zahir A. Daya,[1,2] V. B. Deyirmenjian,[1] and Stephen W. Morris[1]

[1]*Department of Physics, University of Toronto, 60 St. George Street, Toronto, Ontario, Canada M5S 1A7*
[2]*Center for Nonlinear Studies, MS-B258, Los Alamos National Laboratory, Los Alamos, New Mexico 87545*
(Received 30 October 2001; published 18 July 2002)

A sequence of bifurcations is studied in a one-dimensional pattern forming system subject to the variation of two experimental control parameters: a dimensionless electrical forcing number $\mathcal{R}$ and a shear Reynolds number Re. The pattern is an azimuthally periodic array of traveling vortices with integer mode number m. Varying $\mathcal{R}$ and Re permits the passage through several codimension-two (CoD2) points. We find that the coefficients of the nonlinear terms in a generic Landau equation for the primary bifurcation are discontinuous at the CoD2 points. Further, we map the stability boundaries in the space of the two parameters by studying the subcritical secondary bifurcations in which $m \to m+1$ when $\mathcal{R}$ is increased at constant Re.

In typical nonlinear pattern-forming systems, there is one easily adjusted quantity, the control parameter, whose variation results in a symmetry-breaking bifurcation to an ordered pattern [1]. If a second control parameter is available, then it may be possible to tune the parameters to codimension-two (CoD2) points at which two modes with different symmetries are equally unstable. Near such points, neighboring unstable modes compete with one another leading to low-lying secondary bifurcations even in the weakly nonlinear regime that is accessible to perturbative theoretical treatment. There are few experimental systems whose patterns can be conveniently manipulated by the independent variation of two control parameters. Examples include Rayleigh-Bénard convection in a rotating cylinder [2,3], convection in binary fluid mixtures [1,4], and Taylor vortex flow (TVF) with rotation of both the inner and outer cylinders [1,5]. In most cases, the eventual two dimensionality of the patterns results in a very complex phenomenology.

In this Rapid Communication, we study experimentally the bifurcations in a thin annular fluid film that is both sheared and driven into electroconvection [6]. This system is unique in that the bifurcations are produced by two easily adjusted control parameters and are to *strictly* one-dimensional (1D) patterns. The patterns of unidirectionally traveling vortices are distinguished only by their symmetry. The competing patterns in most other fluid-mechanical systems have different symmetries *and* dimensions. For example, in TVF there is a CoD2 point where Taylor and spiral vortices are simultaneously unstable. The former (latter) pattern is 1D and axisymmetric (2D and nonaxisymmetric). The geometry of the TVF fluid system makes it more difficult to examine experimentally how the symmetry versus dimensionality of the competing modes affects physical processes. Our system is free of these dimensionality complications.

Symmetry breaking is the hallmark of a wide array of physical phenomena across many disciplines [1]. The highly restricted geometry of our fluid film allows us to realize experimentally the simplest possible symmetry-breaking transition of a periodic 1D pattern. The primary bifurcation is the transition from the conducting state to a convecting state with m-fold rotational symmetry. The secondary bifurcations connect m to $(m+1)$-fold rotationally invariant convecting

states. All of these states are unidirectionally traveling patterns. Symmetry alone determines the nature of the bifurcations. This scenario can be modeled by coupled Landau amplitude equations that can be calculated completely by perturbative methods from the primitive electrohydrodynamic equations [7,8]. The amplitude equations reduce to a single generic Landau equation when applied to the primary bifurcation. An important aspect of our experiments is the quantitatively determined variation of the coefficients of the nonlinear terms in this equation with a control parameter. We demonstrate that near CoD2 points, the coefficients are discontinuous and the secondary bifurcations are subcritical and suppressed by the second control parameter.

The experimental system consists of an annular, freely suspended film of smectic-*A* liquid crystal. The layered smectic-*A* phase is isotropic and Newtonian for flows in the plane of the film, and maintains a uniform thickness even while flowing. Such a film is driven to electroconvect by a voltage applied between the inner and outer edges that sets up an unstable distribution of surface charge on the film's free surfaces [9]. A Couette shear is applied by mechanical rotation of the inner electrode. Previous studies of this instability explored the behavior of the primary bifurcation to electroconvection [6,9], confirming that the weakly nonlinear regime of convection near onset is described by a complex amplitude equation of the Landau form for a single mode number m [10]. The concentric electrodes have inner (outer) radii r_i (r_o), from which we define the radius ratio $\alpha = r_i/r_o$. The film forms an annular sheet of width $d = r_o - r_i \sim 1$ mm and thickness $s \sim 0.1$ μm so that $s/d \sim 10^{-4}$. The fluid is treated as incompressible, strictly two dimensional, and of uniform electrical conductivity. We denote the fluid density, molecular viscosity, and conductivity by ρ, η, and σ. In a typical experiment, a steady circular Couette shear was imposed by rotating the inner electrode at ω rad/s and a dc voltage V was applied between the inner and outer electrodes. Current-voltage characteristics were obtained for incremental and decremental voltages. The state of the film is specified by the radius ratio and three additional dimensionless parameters. The control parameter $\mathcal{R} = \epsilon_0^2 V^2 / \sigma \eta s^2$, where ϵ_0 is the permittivity of free space, is a measure of the external driving force. The Prandtl-like parameter
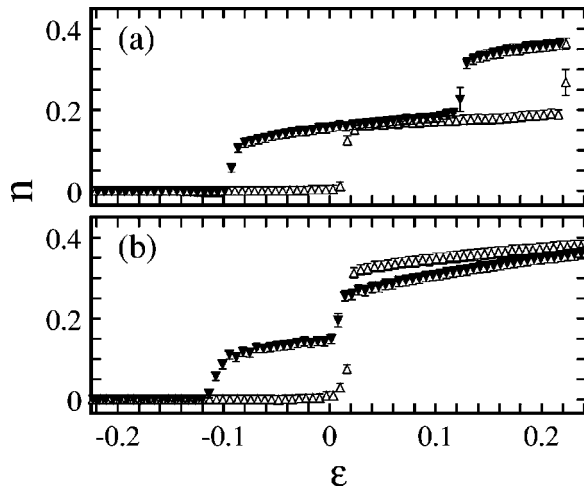
FIG. 1. Plots of n versus ϵ for $\alpha = 0.47$. In (a) $\mathcal{P} = 15.3$, Re $= 0.94$. In (b) $\mathcal{P} = 21.7$, Re $= 0.58$.

$\mathcal{P} = \epsilon_0 \eta / \rho \sigma s d$ is the ratio of the time scales of electrical and viscous dissipation processes in the film. The Reynolds number Re $= \rho \omega r_i d / \eta$ indicates the strength of the applied shear and is the second control parameter. Details of the experimental apparatus and procedure can be found in Refs. [6,9–11].

The primary bifurcation leads to a pattern of m vortex pairs. Onset occurs at a critical voltage $V = V_c$ with the critical mode number $m = m_c$ becoming unstable. Linear stability [9] predicts the values of m_c and the critical control parameter $\mathcal{R}_c \propto V_c^2$ at which the film becomes marginally unstable. In general, $\mathcal{R}_c$ and m_c are functions of α, $\mathcal{P}$, and Re. However, when Re $= 0$, $\mathcal{R}_c = \mathcal{R}_c^0$, and $m_c = m_c^0$ are independent of $\mathcal{P}$. When Re > 0, it is found that $\mathcal{R}_c > \mathcal{R}_c^0$, for any α and $\mathcal{P}$, i.e., that the shear always acts to stabilize the conduction state and suppresses the onset of convection. In addition for nonzero shear, $m_c \lesssim m_c^0$. Both these predictions of linear theory have been experimentally confirmed. Our main experimental tool is the total electric current I, which is a measure of the rate of charge transport due to both conduction and convection. The reduced Nusselt number n is the ratio of the current due to electroconvection to that due to conduction and is defined as $n = (I/I_{cond}) - 1 = (I/cV) - 1$. The conductance of the film c is obtained from the current-voltage characteristic of the film when it is not convecting. Similarly, the reduced control parameter ϵ, is given by $\epsilon = (\mathcal{R}/\mathcal{R}_c) - 1 = (V/V_c)^2 - 1$. The raw (V,I) data can thus be transformed to measurements of (ϵ, n) [12]. In these dimensionless terms, the primary bifurcation occurs at $\epsilon = 0$. When ϵ is increased, the secondary bifurcations are transitions between flows with mode numbers $m \to m + 1$ [13]. Upon decreasing ϵ, the transitions $m \to m - 1$ are observed. The mode changes can be observed directly, but rather crudely, using visual observations of slightly nonuniform films, or films seeded with small particles. They appear very cleanly, if more indirectly, in the form of jumps in n as a function of ϵ. These observations are in qualitative agreement with an equivariant bifurcation theory [14]. Increasing (decreasing) ϵ results in secondary bifurcations at $\epsilon_1 < \epsilon_2 < \cdots$ ($\epsilon_{-1} < \epsilon_{-2} < \cdots$) correspond-
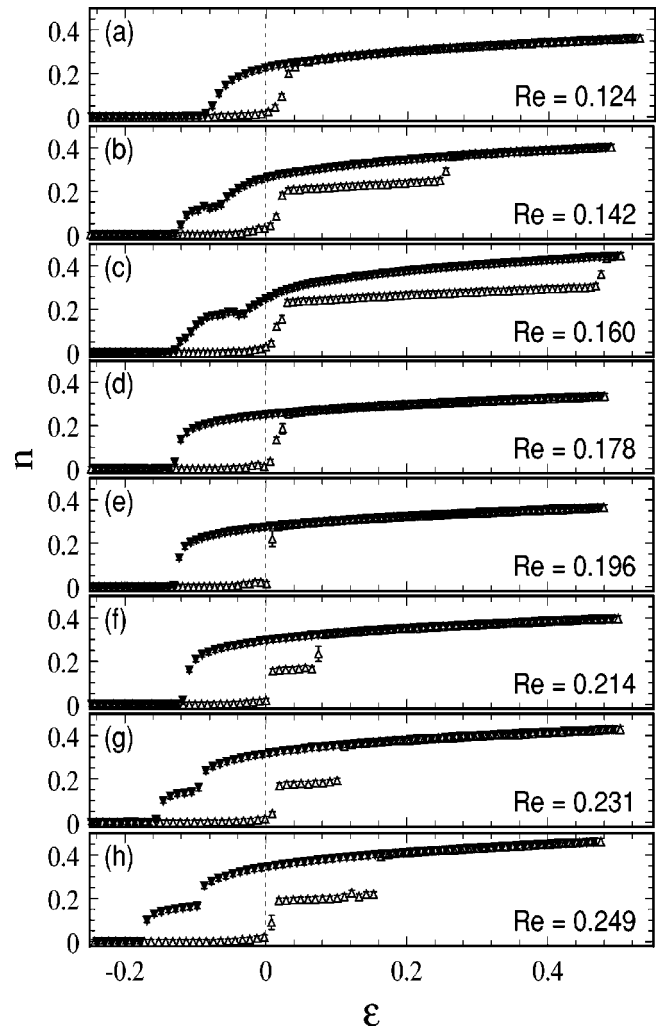

FIG. 2. A Resequence demonstrating mode changing bifurcations. Plotted are n versus ϵ at $\alpha = 0.56$ and $\mathcal{P} = 76$ for a sequence of increasing Re. The open (filled) triangles are for increasing (decreasing) ϵ data.

ing to mode transitions $m \to m + 1 \to \cdots$ ($\cdots \to m + 1 \to m$).

In Fig. 1 are illustrated two representative examples of secondary bifurcations. Figure 1(a) shows (ϵ, n) data for a sheared film with subcritical primary and secondary bifurcations. The secondary bifurcation, which results in one additional traveling vortex pair, appears at $\epsilon_1 \sim 0.22$ for increasing ϵ. When ϵ is decreased, the removal of the vortex pair occurs at $\epsilon_{-1} \sim 0.12$. Convection altogether ceases at $\epsilon \sim -0.1$. Figure 1(b) shows a case where, for increasing ϵ, the primary and secondary bifurcations appear as a single strongly subcritical bifurcation at $\epsilon \sim 0$. However, for decreasing ϵ, ϵ_{-1} is distinct from $\epsilon \sim -0.11$ where convection stops. That shear selects the mode which is linearly unstable is well established in the case of the primary bifurcation [9]. It has been shown from linear stability analysis that the marginally unstable mode decreases from $m_c^0 \to m_c^0 - 1 \to m_c^0 - 2 \cdots$ as Re is increased. Hence, for fixed α and $\mathcal{P}$, there are CoD2 points at particular Reynolds numbers, Re$_{m,m-1}$, at which both m and $m - 1$ are marginally unstable [16]. For Re $<$ Re$_{m,m-1}$, the primary bifurcation is to a convecting

state with mode number m. The first secondary bifurcation occurs at $\epsilon=\epsilon_1>0$ to mode number $m+1$. For Re $>\mathrm{Re}_{m,m-1}$, the primary bifurcation is to mode $m-1$. The first secondary bifurcation is at $\epsilon=\epsilon_1>0$ to mode m. Clearly, it follows that as $\mathrm{Re}\to\mathrm{Re}_{m,m-1}$ from above, $\epsilon_1\to0$, resulting in the situation depicted in Fig. 1(b). Our experimental protocol was always to hold Re constant and vary ϵ. Neither experiment nor theory has addressed the question of what mode transitions occur if Re is varied for constant ϵ.

Figures 2(a)–2(h) show a sequence of (ϵ,n) data plots for $\alpha=0.56$, $\mathcal{P}=76$, and a range of closely spaced values of Re. In Fig. 2(a), the data at $\mathrm{Re}=0.124$ shows a subcritical primary bifurcation with mode number $m=8$. For the range of ϵ investigated, secondary bifurcations were not encountered. In Fig. 2(b), the data at $\mathrm{Re}=0.142$ shows a subcritical primary bifurcation with $m=7$ followed by a subcritical secondary bifurcation $(m=7\to8)$ at $\epsilon_1\sim0.26$. Hence at some Reynolds number, $0.124<\mathrm{Re}_{8,7}<0.142$, there is nascent at $\epsilon=0$ the mode change $8\to7$. At $\mathrm{Re}=0.160$, the secondary bifurcation is suppressed to higher $\epsilon_1\sim0.48$, as shown in Fig. 2(c). The sequence of events in Figs. 2(a) through 2(c) repeats with increasing Re. In Fig. 2(f), data at $\mathrm{Re}=0.214$ shows a primary bifurcation to $m=6$ and a secondary bifurcation at $\epsilon_1\sim0.07$ to $m=7$. Hence a second CoD2 point at $0.196<\mathrm{Re}_{7,6}<0.214$ is traversed. At $\mathrm{Re}=0.231$ and Re $=0.249$, the secondary bifurcation is suppressed to ϵ_1 ~0.11 and $\epsilon_1\sim0.16$ respectively, as is shown in Figs. 2(g) and 2(h). The data obtained while ϵ is being reduced has equally interesting behavior. For example, for increasing ϵ in Fig. 2(f) there is a $m=6\to7$ bifurcation, but for decreasing ϵ the $m=7$ convecting state exits directly to conduction by a single discontinuous transition, without recourse to the $m=6$ state. However, for the slightly higher Re in Figs. 2(g) and 2(h), the $m=6$ state is revisited while ϵ decreases.

For nonzero shear, symmetry and perturbative analyses of the primitive equations lead to the amplitude equation

$$
\begin{aligned}
\tau(\dot{A}_m-ia_{Im}A_m)={}&\epsilon(1+ic_{0m})A_m-g_{0m}(1+ic_{2m})|A_m|^2A_m\\
&-g_{1m}(1+ic_{3m})|A_n|^2A_m\\
&-h_{0m}(1+ic_{4m})|A_m|^4A_m+\cdots,\quad(1)
\end{aligned}
$$

and its counterpart under $m\leftrightarrow n$ symmetry [8]. In the above, all the coefficients are real. The steady state solutions of the real part of Eq. (1) are consistent with the experimental observations of a state m being replaced by a state $n=m\pm1$ via a discontinuous transition [8]. To further interpret the data in Fig. 2 and better understand the behavior of the primary bifurcation as the Reynolds number is increased through $\mathrm{Re}_{8,7}$ and $\mathrm{Re}_{7,6}$, we consider the real and steady state part,

$$
\epsilon A-gA^3-hA^5=0,\quad(2)
$$

of Eq. (1), where A is real, $g\equiv g_{0m}$, and $h\equiv h_{0m}$. We have truncated at quintic order in the expansion. Since the reduced Nusselt number $n=A^2$ [7,10], we can determine g and h for each primary bifurcation in the sequence in Fig. 2. Our results are plotted in Fig. 3. We find that both g and h are strongly discontinuous as Re is increased through the CoD2
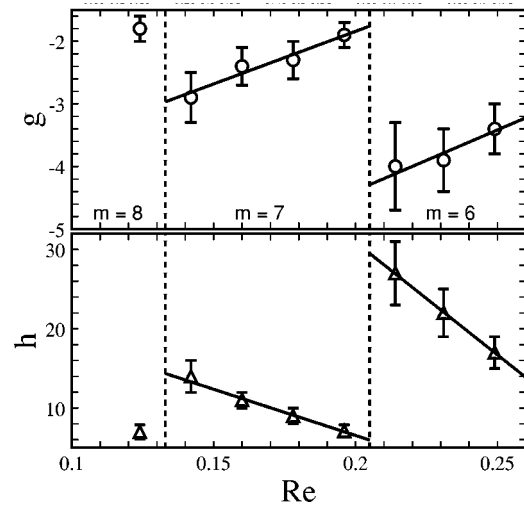

FIG. 3. The coefficients g and h versus Re for the data in Fig. 2. The dashed lines locate the CoD2 points. The solid lines are linear fits to the data.

points $\mathrm{Re}_{8,7}$ and $\mathrm{Re}_{7,6}$. The discontinuity in both g and h is smaller at $\mathrm{Re}_{8,7}$ than at $\mathrm{Re}_{7,6}$. This raises the possibility that these discontinuities may vanish in the limit $m\to\infty$ and so are a feature of the finite size and discrete mode structure of this system.

A minimal description of a state consists of identifying the value of its mode number m. Allowing for hysteresis, each state persists over certain overlapping ranges of α, $\mathcal{P}$, $\mathcal{R}$, and Re. Here, we focus on fixed α and $\mathcal{P}$ for simplicity
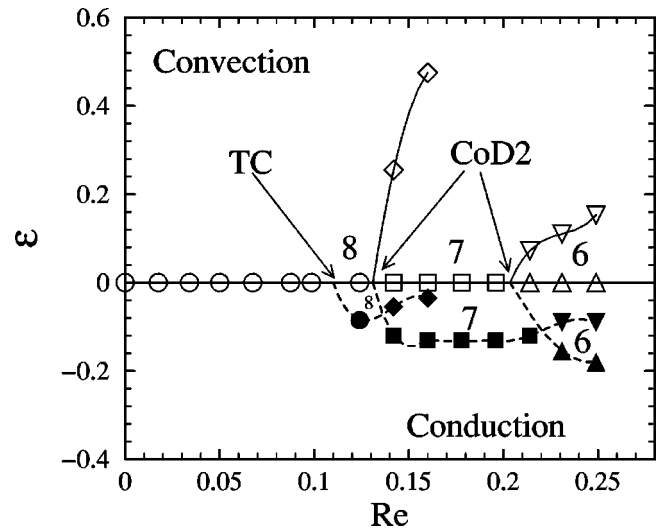

FIG. 4. Plot of the parameter space of patterns with mode numbers m for $\alpha=0.56$ and $\mathcal{P}=76$. Open (closed) symbols indicate conduction$\to m$ ($m\to$conduction) and $m\to m+1$ ($m+1\to m$) transitions encountered for increasing (decreasing) ϵ. The numbers are the observed m. The region below (above) $\epsilon=0$ is multistable with conduction (m and $m+1$ states). TC is a tricritical point that connects the supercritical and subcritical branches. CoD2 are codimension-two points. The solid lines for $\epsilon>0$ are the secondary stability boundaries across which $m\to m+1$. Each of the dashed lines for $\epsilon<0$ connects the positions of the saddle nodes for mode m.

[15]. In Fig. 4 we map the solutions in the subspace defined by (ϵ, Re, $\alpha = 0.56$, $\mathcal{P} = 76$), where the reduced variable ϵ is used for convenience. Figure 4 shows the values of ϵ at which conduction and convection with various m were found, for given values of Re. Below (above) the lowermost dashed lines (horizontal solid line), only conduction (convection) occurs. Between these lines both conduction and convection are observed, depending hysteretically on whether ϵ is increasing or decreasing. A tricritical point (TC) is shown at Re ~ 0.11. For Re $\lesssim 0.11$ the onset of convection is supercritical and hence nonhysteretic [10].

Within the convecting regime, the boundaries of the secondary bifurcations between $m = 8,7$ and $m = 7,6$ show upwards trends indicating that an analogous suppression occurs for the modes $m = 8$ and $m = 7$, even after they cease to be the primary mode of bifurcation [17]. The suppression of the secondary modes increases more rapidly with Re than when they were the primary mode, with larger m modes suppressed more rapidly than smaller m modes. Inside the hysteresis loop of the primary bifurcation, we found as many as three possible distinct states, one being conduction. [See Figs. 2(b), 2(c), 2(g), and 2(h).] The entire portrait presented in Fig. 4 depends perhaps strongly on α and weakly on $\mathcal{P}$ and is likely to be more branched (contain more transitions) for larger α. It should be possible to generate theoretically such a tree from the primitive equations, once they have been reduced to the form of Eq. (1) [8].

We have shown that in our discrete-mode system, secondary bifurcations appear near CoD2 points. Using a generic Landau model, we have quantitatively analyzed the behavior of the primary bifurcations on either side of these points. We have found that the coefficients of the cubic and quintic terms of the Landau equation are strongly discontinuous at the CoD2 points. We expect that this scenario occurs over large regions of our parameter space and may well be a general property of discrete-mode pattern-forming systems such as TVF [5]. Unlike TVF however, this system only has bifurcations between one-dimensional patterns with simple m-fold rotational symmetries. The parameter space is characterized by branches that demarcate different stable and multistable domains. The surprisingly intricate bifurcation structure of this highly geometrically constrained instability is amenable to detailed quantitative analysis starting from the underlying electrohydrodynamic equations [8]. As such, it is an ideal venue for experimental and theoretical studies of bifurcations in finite nonlinear pattern-forming systems.

[1] M.C. Cross and P.C. Hohenberg, Rev. Mod. Phys. **65**, 851 (1993).

[2] Y. Liu and R.E. Ecke, Phys. Rev. E **59**, 4091 (1999).

[3] F. Zhong, R.E. Ecke, and V. Steinberg, Phys. Rev. Lett. **67**, 2473 (1991).

[4] I. Rehberg and G. Ahlers, Phys. Rev. Lett. **55**, 500 (1985).

[5] P. Chossat and G. Iooss, *The Couette-Taylor Problem* (Springer, New York, 1994).

[6] Z.A. Daya, V.B. Deyirmenjian, S.W. Morris, and J.R. de Bruyn, Phys. Rev. Lett. **80**, 964 (1998).

[7] V.B. Deyirmenjian, Z.A. Daya, and S.W. Morris, Phys. Rev. E **56**, 1706 (1997).

[8] V.B. Deyirmenjian, Z.A. Daya, and S.W. Morris (unpublished).

[9] Z.A. Daya, V.B. Deyirmenjian, and S.W. Morris, Phys. Fluids **11**, 3613 (1999).

[10] Z.A. Daya, V.B. Deyirmenjian, and S.W. Morris, Phys. Rev. E **64**, 036212 (2001).

[11] Z.A. Daya, Ph. D. thesis, University of Toronto, 1999.

[12] V_c is determined by fitting the (ϵ,n) data to the appropriate Landau amplitude equation. See Refs. [10] and [11].

[13] Mode transitions $m \rightarrow m \pm n$ with $n > 1$ are unlikely except at large α.

[14] W.F. Langford and D.D. Rusu, Physica A **261**, 188 (1998).

[15] $\mathcal{P}$ slowly varied by less than 2% [10,11] over the course of a run due to the electrochemical drift of the electrical conductivity of the liquid crystal.

[16] It is also possible to reach CoD2 points by tuning α even for Re $= 0$. Codimension-three or -four points, though unlikely, are possible since ϵ, Re, α, and $\mathcal{P}$ are all tunable.

[17] The suppression of the primary mode is set to zero by the definition of ϵ.